

Machine Learning Assisted Extraction of Vertical Cavity Surface Emitting Lasers Parameters

Original

Machine Learning Assisted Extraction of Vertical Cavity Surface Emitting Lasers Parameters / Khan, I., Tunesi, L., Masood, M.U., Ghillino, E., Carena, A., Curri, V., Bardella, P.. - ELETTRONICO. - (2022), pp. 1-2. (2022 IEEE Photonics Conference (IPC) Vancouver, BC, Canada 13-17 November 2022) [10.1109/IPC53466.2022.9975585].

Availability:

This version is available at: 11583/2976007 since: 2023-02-14T09:07:16Z

Publisher:

IEEE

Published

DOI:10.1109/IPC53466.2022.9975585

Terms of use:

This article is made available under terms and conditions as specified in the corresponding bibliographic description in the repository

Publisher copyright

IEEE postprint/Author's Accepted Manuscript

©2022 IEEE. Personal use of this material is permitted. Permission from IEEE must be obtained for all other uses, in any current or future media, including reprinting/republishing this material for advertising or promotional purposes, creating new collecting works, for resale or lists, or reuse of any copyrighted component of this work in other works.

(Article begins on next page)

Machine Learning Assisted Extraction of Vertical Cavity Surface Emitting Lasers Parameters

Intesham Khan*, Lorenzo Tunesi*, Muhammad Umar Masood*, Enrico Ghillino[†],
Andrea Carena*, Vittorio Curri* and Paolo Bardella**

*Department of Electronics and Telecommunications, Politecnico di Torino, Torino, Italy

[†]Synopsys Inc., Ossining, NY 10562, USA

**paolo.bardella@polito.it

Abstract

We propose a machine learning-based framework to extract circuit-level VCSEL model parameters. The proposed approach predicts the parameters exploiting the light-current curve and small-signal modulation responses with two steps at constant and variable temperature, respectively. Promising results are achieved in terms of relative prediction error.

Keywords

Vertical Cavity Surface Emitting Lasers, Machine Learning, Parameters extraction, Circuit-level models, Deep Neural Network.

I. INTRODUCTION

In the last decades, many computationally efficient models have been introduced to describe both stationary and dynamic Vertical Cavity Surface Emitting Lasers (VCSEL) behaviors accurately. These models play a fundamental role in understanding the VCSEL physical properties, allowing further optimizations of these devices. Along with this, they are also an essential resource for performing a realistic simulation of VCSEL sources as part of larger optoelectronic systems. Indeed, so-called "circuit-level models" of VCSEL are available in simulation tools such as Synopsys OptSim circuit simulation environment [1]. However, in these models, many physical parameters must be appropriately set to accurately reproduce the behavior of existing laser sources, which is a necessary step to obtain correct results from the numerical simulation of a whole photonic system. The extraction of these unknown physical parameters from experimental curves is generally time-consuming and relies, e.g., on trial and error approaches or regression analysis. In this scenario, we propose a Machine learning (ML) based approach to the problem, which is able to extract the required VCSEL parameters from experimental data effectively.

II. VCSEL MODEL

The considered VCSEL model, available as a standard OptSim block, is an extension of the model originally proposed in [2] to include the temporal evolution of the field phase [3]. In cylindrical geometry, the carriers number is expanded in Bessel series and the first two terms N_0 and N_1 are considered [4]. Assuming spatially independent rate equations, Eq.s 1-4 can be introduced for the temporal evolution of the carriers N_0 and N_1 , the photons number S and the phase ϕ , with I injected current, q electron charge, I_1 leakage current, ϕ_{100} and ϕ_{101} overlap coefficient, β spontaneous emission coefficient, α linewidth enhancement factor. In order to model the dependence of the VCSEL behavior with respect to temperature T , a phenomenological representation of the gain G and the carrier transparency number N_t is introduced based on fitting parameters, as shown in Eq.s 5-6 [2]. Other parameters introduced in Eq.s (1-6), objective of the ML study, are finally defined in Tables I and II.

$$\frac{dN_0}{dt} = \frac{\eta_i I}{q} - \frac{N_0}{\tau_n} - \frac{G[\gamma_{00}(N_0 - N_t) - \gamma_{01}N_1]}{1 + \varepsilon S} S - \frac{I_1}{q} \quad (1) \quad \frac{dN_1}{dt} = -\frac{N_1}{\tau_n}(1 + h_{\text{diff}}) + \frac{G[\phi_{100}(N_0 - N_t) - \phi_{101}N_1]}{1 + \varepsilon S} S \quad (2)$$

$$\frac{dS}{dt} = -\frac{S}{\tau_p} + \frac{\beta N_0}{\tau_n} + \frac{G[\gamma_{00}(N_0 - N_t) - \gamma_{01}N_1]}{1 + \varepsilon S} \quad (3) \quad \frac{d\phi}{dt} = \frac{\alpha G[\gamma_{00}(N_0 - N_t) - \gamma_{01}N_1]}{2(1 + \varepsilon S)} \quad (4)$$

$$G(T) = G_0 (a_{g0} + a_{g1}T + a_{g2}T^2) / (b_{g0} + b_{g1}T + b_{g2}T^2) \quad (5) \quad N_t(T) = N_{tr} (c_{n0} + c_{n1}T + c_{n2}T^2) \quad (6)$$

III. MACHINE LEARNING AND DATASET GENERATION

The proposed analysis focuses the extraction of 18 parameters listed in Tables I and II. The complexity of the analysis is reduced by executing it in a two-step approach, which requires the training of two smaller ML agents mainly based on a Deep neural network (DNN) architecture having three hidden layers with ten neurons per layer [5]. The proposed DNN model used ReLU as an activation function and Mean square error (MSE) as a loss function. The DNN model is configured for 100 training steps with a default learning rate of 0.01. The training and test set proportion is 70% and 30% of the total dataset.

The first DNN agent is trained using data generated at a constant temperature and is used to extract the experimental data parameters reported in Table I. In particular, a dataset of 10000 simulations is created at the constant temperature of 25 °C, changing the values of parameters listed in Table I and keeping all the other parameters fixed; parameters appearing in Table II

Parameter	Range	Value
Current injection η_i	0.4 to 1	0.8
Photons lifetime τ_p	1.5 ps to 3.5 ps	2.5 ps
Carrier lifetime τ_n	1.5 ns to 3.5 ns	2.5 ns
Gain coefficient g_0	$25\,000\text{ s}^{-1}$ to $75\,000\text{ s}^{-1}$	$50\,000\text{ s}^{-1}$
Carrier transparency number n_{tr}	0.5×10^6 to 1.5×10^6	1×10^6
Gain saturation factor ϵ	3×10^{-7} to 6×10^{-7}	5×10^{-7}
Overlap coeff. ($N_0 - S$) γ_{00}	0.75 to 1	1
Overlap coeff. ($N_0 - S$) γ_{01}	0.2 to 0.5	0.38
Diffusion parameter h_{diff}	7.5 to 22.5	15

TABLE I: Parameters investigated and variation ranges for generating 1st dataset at 25 °C. Last columns values were elected for generating 2nd dataset.

Parameter	Range
Gain coeff. parameter a_{g0}	-0.6 to -0.2
Gain coeff. parameter a_{g1}	$1 \times 10^{-3}\text{ K}^{-1}$ to $3 \times 10^{-3}\text{ K}^{-1}$
Gain coeff. parameter a_{g2}	$3 \times 10^{-7}\text{ K}^{-2}$ to $3 \times 10^{-8}\text{ K}^{-2}$
Gain coeff. parameter b_{g0}	0.5 to 3
Gain coeff. parameter b_{g1}	$-5 \times 10^{-3}\text{ K}^{-1}$ to $-2 \times 10^{-3}\text{ K}^{-1}$
Gain coeff. parameter b_{g2}	$1 \times 10^{-5}\text{ K}^{-2}$ to $3 \times 10^{-5}\text{ K}^{-2}$
Transparency number param. c_{n0}	-0.5 to -2
Transparency number param. c_{n1}	$4 \times 10^{-3}\text{ K}^{-1}$ to $1.2 \times 10^{-2}\text{ K}^{-1}$
Transparency number param. c_{n2}	$3 \times 10^{-6}\text{ K}^{-2}$ to $1.2 \times 10^{-5}\text{ K}^{-2}$

TABLE II: Parameters investigated and variation ranges for generating the 2nd dataset.

are set at their central value of the proposed ranges while other parameters use the default values indicated in OptSim. For each set of parameters, the dataset is filled with 16 samples of the calculated Light-Current (L-I) curve, generated for linearly spaced injected currents I ranging from 1 mA to 25 mA, an interval compatible with the considered parameter ranges. Also, small-signal modulation responses are calculated at 6 mA, 12 mA, 18 mA, and 24 mA; for each curve 16 samples are saved, for frequencies logarithmically spaced between 10 kHz and 50 GHz. Once the first agent is trained and the first set of parameters has been extracted matching the experimental data of interest (resulting, e.g., in the values indicated in the last column of Table I), the second DNN agent is trained using L-I curves calculated at different temperatures changing the parameters listed in Table II, all introducing a dependence of gain and transparency carrier number with temperature. A second ML agent can then be used to calculate the optimal values of those parameters according to the experimentally measured data. For this second analysis, a new dataset of 10 000 simulations is generated, containing the data from 4 L-I curves calculated at 10 °C, 25 °C, 40 °C, and 55 °C; for each L-I curve 16 samples are stored which are used to train the second DNN agent.

IV. RESULTS AND CONCLUSION

The relative error of the considered parameters in the first and second test sets are presented in Fig. 1 and Fig. 2, respectively. For all the listed parameters, the corresponding MSE at the end of the training is less than 0.1. In general, extremely high accuracy is obtained for the 9 parameters considered in the first step of the procedure, while a less accurate prediction is achieved for some of the parameters introducing the temperature dependence, such as a_{g2} and c_{n2} . However, the latter coefficients introduce a second-order dependence with temperature, which causes limited effects over the considered temperature range, and are therefore difficult to estimate. Overall, the proposed procedure can extract an accurate set of VCSEL parameters through a fully automatized process that requires approximately one hour of calculation on a modern laptop for the generation of the datasets and the ML training. Furthermore, the proposed procedure can be easily expanded to consider a larger number of parameters (with respect to the 18 analyzed in this work) in more complex models and can be definitely adapted to the study of other laser families.

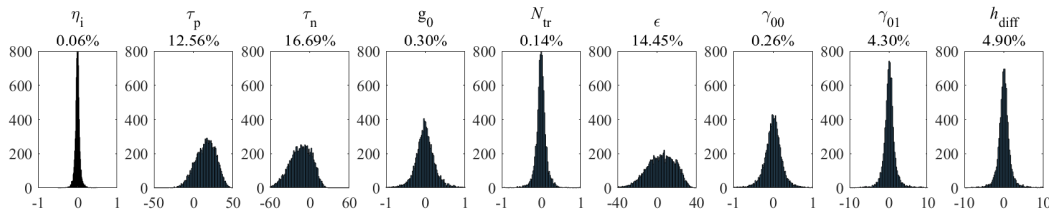


Fig. 1: Relative predicting error of 1st agent for the 9 considered parameters. Values in the titles of each histogram indicate the relative error standard deviation.

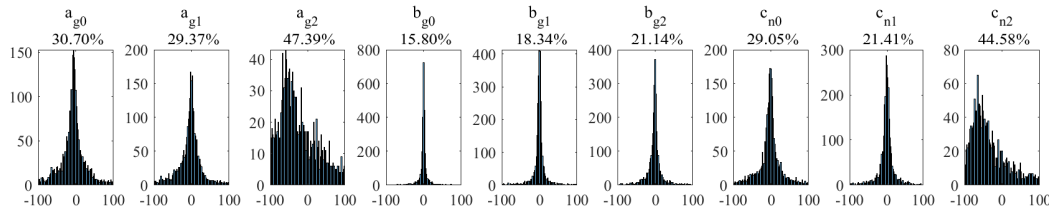


Fig. 2: Relative predicting error of 2nd agent for the 9 considered parameters. Values in the titles of each histogram indicate the relative error standard deviation.

REFERENCES

- [1] <https://www.synopsys.com/photonic-solutions/pic-design-suite.html>.
- [2] P. Mena *et al.*, "A comprehensive circuit-level model of vertical-cavity surface-emitting lasers," *JLT*, vol. 17, no. 12, pp. 2612–2632, 1999.
- [3] M. Jungo *et al.*, "Vistas: a comprehensive system-oriented spatiotemporal vcsel model," *IEEE JSTQE*, vol. 9, no. 3, pp. 939–948, 2003.
- [4] P. Mena *et al.*, "Compact representations of mode overlap for circuit-level vcsel models," in *IEEE LEOS 2000*, vol. 1, 2000, pp. 234–235 vol.1.
- [5] I. Khan *et al.*, "A neural network-based automatized management of $n \times n$ integrated optical switches," in *Photonic Networks and Devices*. OSA, 2021, pp. NeF2B–2.